International Journal of Solids and Structures 49 (2012) 2617–2624

Contents lists available at SciVerse ScienceDirect

International Journal of Solids and Structures

journal homepage: www.elsevier.com/locate/ijsolstr

Biological membranes from the perspective of smart materials – A theoretical study

Lior Atia, Sefi Givli *

Faculty of Mechanical Engineering, Technion – Israel Institute of Technology, Haifa 32000, Israel

ARTICLE INFO

Article history:
Received 1 June 2011
Received in revised form 27 March 2012
Available online 12 June 2012

Keywords:
Bio-materials
Lipid
Stability
Equilibrium
Heterogeneous
Deflection
Spontaneous curvature

ABSTRACT

The unique properties and diverse functionality of biological membranes make them excellent candidates for nano-scale applications, such as sensors and actuators. Taking the view of biological membranes as smart bio-materials, we study the behavior of a simply supported beam made from a biological membrane-like material. Equilibrium configurations are derived by calculating the first variation of a generalized Helfrich energy, and their stability is examined by means of the second variation. Our numerical results demonstrate the richness of phenomena exhibited by these structures, in accordance with experimental observation of multi-component vesicles. Further, we demonstrate that the intriguing behavior of biological membrane beams, which is fundamentally different from standard beams and from standard Cahn Hilliard systems, can be utilized for actuation and sensing. For example, temperature and also pressure difference across the membrane can be indirectly measured by gauging the fluorescence intensity of the membrane components.

1. Introduction

The rapid progress in nano-scale technologies along with new findings in the behavior of biological systems emphasize the potential in integrating bio-materials into nano-scale engineering applications and in developing bio-inspired materials. From the engineering perspective, efforts are under way to manufacture devices at ever smaller sizes. These efforts have reached the point where it is required that materials act as "machines" themselves, i.e., provide functions such as actuation and sensing without the need of moving parts or complicated structures (Bhattacharya and James, 2005). For this reason, the interest in "intelligent" materials, which can undergo reversible deformations in response to external stimuli, such as temperature, pressure, PH, magnetic field (or alternatively sense changes in these quantities) is constantly increasing. An important class of such materials are adaptive materials, which experience significant changes in their mechanical properties in response to external stimuli, and vice-versa. A classic example are materials undergoing martensitic phase transformations, such as shape memory alloys and magnetostrictive alloys (James and Hane, 2000). These materials can provide large deformations which are attributed to "switching" (or transformations) between different locally stable configurations at the level of the atomic lattice.

In this paper we introduce the concept of using biological membranes as adaptive materials for applications at the nano-scale. Specifically, we propose to utilize the unique properties and diverse functionality of the biological membrane (BM) to provide sensing of temperature and osmotic pressure, as well as actuation in response to external stimuli. Besides the new and exciting possibilities they provide, a main advantage of the BMs is their bio-compatibility which makes them natural candidates for applications associated with invasive medical applications or study of biological systems. In addition, we show that one can take advantage of the adaptive nature of biological membranes in order to indirectly measure some of the non-standard material properties of the membrane.

Biological membranes play a crucial role in a wide range of biological processes. As fundamental building blocks of cell walls, mitochondria and numerous other important cell organelles, they protect by providing a barrier, control transport, dominate cell to cell recognition, cell adhesion, and more. Despite their diverse functionality, the BMs are fairly simple in construction. They are made from (phospho) lipid molecules and functional molecules (mostly proteins). The lipid molecules are composed of a hydrophilic ("water loving") head group and a hydrophobic ("water hating") tail. When the lipid molecules are put in water in the right concentration, this conflict is beautifully resolved by the formation of a lipid bilayer, which is energetically (free energy) most favorable. The lipid bilayer provides the basic structure and serves as a permeability barrier, while the proteins molecules mediate most of the other functions of the membrane, and may act as receptors, "pumps", "channels" and more. BMs from different cells can differ widely both in the relative amounts and in the types of their constituent proteins and lipids (Swanson and Webster, 1977). This

* Corresponding author.
E-mail address: givli@technion.ac.il (S. Givli).

0020-7683/$ - see front matter © 2012 Elsevier Ltd. All rights reserved.
http://dx.doi.org/10.1016/j.ijsolstr.2012.05.030

variation is the basis for the wide range of biological activities displayed by different membranes.

A consequence of the bilayer construction is that it is rather floppy, i.e., it is more susceptible to bending rather than stretching (Boal, 2002). In addition, BMs can resist stretching but not shear, and its constituent molecules can move relatively easy within the membrane. This suggests a fluid-like nature, first introduced in 1972 by Singer and Nicolson (Singer and Nicolson, 1972) as the "fluid mosaic" model. New findings in the past four decades have led to an amended version of the "fluid mosaic" model which now includes considerable variations in bilayer thickness, domains with high concentrations of proteins, and patchiness in the membrane plane (Engelman, 2005).

An important avenue through which BMs achieve their diverse functionality is through strong coupling between membrane mechanics and biochemical events. Generally speaking, mechanical "signals", carried by the membrane, are preconditioning for the onset of many biochemical events in the cell, and have an important role in controlling and regulating cell biochemistry (Ingber, 2006; Perozo and Rees, 2003; Stamenovic and Wang, 2000; Vogel and Sheetz, 2006; Zhu et al., 2000). The coupling between biochemical events and mechanics is mediated through two main coupled mechanical processes: deformations (or stresses) and phase segregation. As mentioned earlier, BMs are not made from lipid molecules only, but also from proteins, "rigid" cholesterol molecules and other functional molecules. Moreover, for the same lipid, various bilayer phases may be found, such as gels, liquid disordered and liquid ordered phases. These phases differ in their mechanical properties, leading to a complex heterogeneous mechanical structure. Depending on the types of lipids and the functional molecules involved, as well as the external conditions (such as osmotic pressure, external forces, temperature and level of acidity), the BM can remain homogeneous or segregate into different phases. The latter changes the stress distribution in the membrane and either absorb or release energy. Therefore, just like other heterogeneous materials, deformation of the membrane is affected by composition (Altus and Givli, 2003; Givli and Altus, 2003). However, unlike standard heterogeneous materials structures, composition is modulated by curvature of the membrane. Hence, BMs may be conceived as dynamic structures in the sense that their chemical composition and molecular arrangements responds to changing conditions. The richness of this phenomenon has been demonstrated by several experimental groups (Baumgart et al., 2003, 2005; Kahya et al., 2003; Samsonov et al., 2001; Veatch and Keller, 2003). Furthermore, the shape of the membrane and its bio-chemical function are dominated by the interplay between lipids and proteins: reversible insertion of proteins that act on the membrane like wedges lead to areas with high curvature. In addition, certain types of functional proteins concentrate in domains of curvature that they prefer, leading to the formation of functionalized domains (Sprong et al., 2001). The formation of such domains controls membrane transport, cellular sensors, cellular signaling, and adhesion.

Since the pioneering work of Helfrich (1973), the mechanics of BMs has been studied theoretically extensively (e.g., Evans and Skalak, 1980; Seifert et al., 1991; Zhong-can and Helfrich, 1989). Yet, much of it has focused on single component (homogenous) membranes. In the last two decades there has been a growing effort in studying multi-component BMs theoretically. These works usually focus on specific problems of interest, commonly motivated by a particular experiment, for which various simplifying assumptions can be employed. For example, (Seifert, 1993) studied shape transformation in two-component axisymmetric vesicles by mapping the energy of the two-component system onto the energy of a single-component system. To this end, the non-linear and the gradient composition-related terms have been assumed negligible. Other works commonly assume that the two-component mixture is in the strong segregation limit (Baumgart et al., 2005; Boulbitch, 1999; Harden et al., 2005; Julicher and Lipowsky, 1993; Kawakatsu et al., 1993; Yanagisawa et al., 2010), that one of the components is ideally stiff (Auth and Gompper, 2009), or that the membrane shape is predetermined (Kozlov et al., 1997; Parthasarathy et al., 2006). Also, the stability of equilibrium solutions associated with multi-component BMs has rarely been addressed (Givli et al., 2012; Safran et al., 1991; Veksler and Gov, 2007). Due to the complexity of calculating equilibrium configurations of multi-component and three-dimensional BMs, advanced numerical methods such as nonlinear finite elements and phase field methods have been developed (Du et al., 2004; Feng and Klug, 2006; Lowengrub et al., 2009; Ma and Klug, 2008). The focus of these works is usually put on the numerical procedure.

In this paper we study the behavior of a beam made of a BM-like material, which is simply supported at the beam ends. We consider a BM composed of two components. Equilibrium equations and stability conditions are obtained by calculating the first and second variations of a generalized Helfrich energy functional, subjected to the constraint that the overall composition, i.e., total number of molecules of each type, does not change in the course of the experiment. The energy functional accounts for the elastic energy of the BM, free energy of mixing, coupling between shape and composition through the spontaneous curvature, and arbitrary distribution of the mechanical load exerted on the BM. We calculate equilibrium configurations numerically, and study their stability. Unlike other theoretical studies in the field, which commonly focus on reproducing qualitative observations of specific experiments, the main objective of this paper is to examine the suitability of BMs for engineering applications, such as sensors and actuators. We emphasize that our study is purely theoretical and does not pretend to provide a proof of concept. The main purpose of the paper is to demonstrate the richness of possibilities and to inspire. It is not clear at this point whether integrating BMs into engineering applications can be realized. Yet, we hope that the results presented here will motivate experimental study in this direction.

2. Theoretical considerations

Consider a simply supported beam of length L and width $b \ll L$, as illustrated in Fig. 1. The beam, made of a BM material, is subjected to a distributed load (force per unit area), $q(x)$. We assume that the BM is composed of two components, which we shall refer to as type-I and type-II. These can represent two different lipid phases (e.g., liquid ordered and liquid disordered phases), two different types of lipid molecules, or mobile membrane proteins

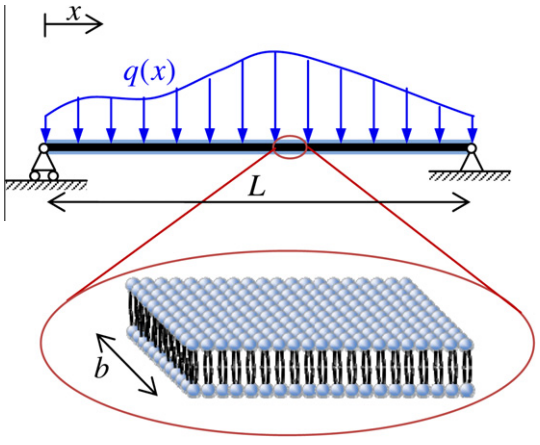

Fig. 1. A simply supported beam (held up by pivot supports at its ends) subjected to a distributed load $q(x)$. The beam is made from a lipid bi-layer comprised from two components. Typical thickness of a bi-layer is five nm, $b \ll L$.

embedded in a lipid phase. We introduce a concentration $c : x \to [0,1]$ which describes the mole fraction of type-I in each point of the beam. Also, we denote by ρ the total density (both phases combined) which describes the number of molecules per area. Since the BM is not susceptible to stretching it is reasonable to assume that ρ is constant. It follows that at any point in the beam, $c\rho$ and $(1-c)\rho$ are the densities of type-I and type-II, respectively. Further, if M_I and M_{II} denote the total number of molecules of each phase, we have

$$\int_L c\rho\, dx = M_I \quad \text{and} \quad \int_L \rho\, dx = M \quad (M \equiv M_I + M_{II}). \tag{1}$$

Above, it was assumed that the densities of the two components are identical. This is commonly a reasonable assumption (Kozlov et al., 1997). However, in certain cases, such as liquid ordered and liquid disordered phases of certain lipids, this may not be the case. Finally, the total potential energy of the vesicle may be written as

$$F = b\int_{x=0}^{L} \varphi\, dx - b\int_{x=0}^{L} qw\, dx; \quad \varphi = f_s(\rho) + f_b(H,c) + f(c) + k_c|\nabla c|^2. \tag{2}$$

Here, the second integral describes the work of the external load, where w is the deflection (vertical displacement) field. Also, f_s and f_b account for the stretching energy and bending energy of the membrane, respectively, f describes the interaction energy between the two phases, H is the mean curvature, and the term $k_c|\nabla c|^2$ penalizes sharp changes in concentration as for example phase boundaries. The function $f : [0,1] \to \mathbb{R}$ is convex at high temperatures (miscible) but non-convex with a double-well structure at low temperatures. Next, we assume that ϕ takes a generalized Helfrich form (Zhong-can and Helfrich, 1989), thus

$$\varphi = \frac{1}{2}k(c)\cdot(2H - H_0(c))^2 + f(c) + \frac{1}{2}k_c|\nabla c|^2, \tag{3}$$

where κ is the bending (mean curvature) modulus and H_0 is the spontaneous curvature. Above, the stretching energy has been ignored since its contribution to the energy is constant. In what follows we assume small deflections. Thus, the mean curvature can be approximated by the second derivative of w with respect to x:

$$2H \cong w_{,xx}. \tag{4}$$

The spontaneous curvature. If the two phases have different molecular structure, any inhomogeneity induces a local spontaneous curvature (see Fig. 2). Therefore, spontaneous curvature is dictated by composition, resulting in a coupling between composition and shape. For example, membrane proteins can act on the membrane as wedges lead to areas of high curvature. Also, different types of lipids can have different molecular shapes. For example, in phosphatidylcholine the headgroup and lipid backbone have similar cross-sectional areas, and therefore the molecule has a cylindrical shape. On the other hand, phosphatidylethanolamine molecules have a small headgroup and are cone-shaped, while in lysophosphatidylcholine the hydrophobic part occupies a relatively smaller surface area and the molecule has the shape of an inverted cone (Sprong et al., 2001). The mixture of cylindrical lipids and conical lipids will have a spontaneous curvature that depends on the concentration of the conical lipids (Das et al., 2008). For simplicity, we assume here that the spontaneous curvature has a linear dependence with concentration, i.e.,

$$H_0(c) = K_c(c - c_0). \tag{5}$$

Above, c_0 is a constant which can take either positive or negative values. If positive, c_0 can be interpreted as the concentration for which the spontaneous curvature is zero (the beam tends to be straight). When negative, the spontaneous curvature is never zero.

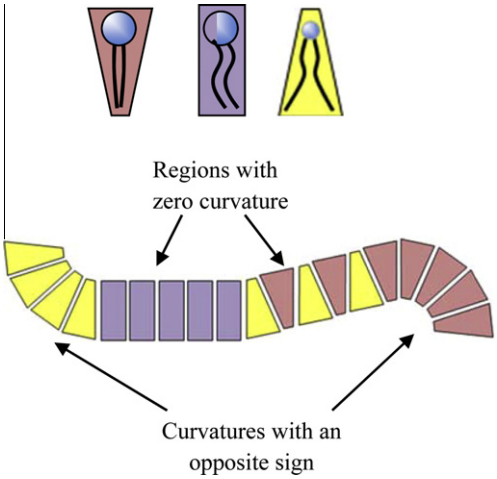

Fig. 2. The molecular shape of lipids determines the spontaneous curvature of the membrane (figure is schematic and not in scale). The shape of a lipid depends on the relative size of its headgroup and tails. In cases where the headgroup and lipid backbone have similar cross-sectional areas, the molecule has a cylindrical shape. Differences in the relative size of the headgroup and tales result in either cone-shape or inverted-cone shape.

2.1. Non-dimensional analysis

We define the unit length as the beam length, L. Accordingly, we introduce the following non-dimensional quantities and operators:

$$\tilde{w} = \frac{w}{L}, \quad (\,)_{,\tilde{x}} = L(\,)_{,x}, \quad \tilde{H}_0 = LH_0. \tag{6}$$

and

$$\tilde{k} = \frac{k}{k^*}, \quad \tilde{k}_C = \frac{k_C}{k^*}, \quad \tilde{q} = q\frac{L^3}{k^*}, \quad \tilde{f} = f\frac{L^2}{k^*}. \tag{7}$$

where $k^* = k|_{c=0.5}$. Therefore, the non-dimensional energy functional reads

$$\tilde{F} = \frac{L}{b}\frac{F}{k^*} = \int_{x=0}^{1}\left(\frac{1}{2}\tilde{k}(\tilde{w}_{,\tilde{x}\tilde{x}} - \tilde{H}_0(c))^2 + \tilde{f}(c) + \frac{1}{2}\tilde{k}_c(c_{,\tilde{x}})^2 - \tilde{q}\tilde{w}\right)d\tilde{x}. \tag{8}$$

In what follows all quantities are non-dimensional, and we disregard the $(\tilde{})$ symbol for brevity.

2.2. Equilibrium equations

We assume that equilibrium configurations of the beam are stationary points of the energy with respect to variations in w and c, subjected to the constraints (1). We note that only the first constraint has to be considered since ρ is constant, and term this constraint the "mass constraint":

$$\int_{x=0}^{1} c\, dx = m_I. \tag{9}$$

where $m_I \equiv \frac{M_I}{M}$ is the average (or total) concentration of type-I. Next, we introduce the following Lagrange functional:

$$F^* = \int_{x=0}^{1}\left(\frac{1}{2}k(w_{,xx} - H_0(c))^2 + f(c) + \frac{1}{2}k_c(c_{,x})^2 - qw\right)dx - \mu\left(\int_{x=0}^{1} c\, dx - m_I\right), \tag{10}$$

where μ is a Lagrange multiplier associated with the mass constraint. Equilibrium equations can be derived by requiring that the first variation of F^* vanishes for *any variation* of w and c. Therefore, we require that

$$\delta^{(1)}F^*(w,c) \equiv \lim_{\varepsilon \to 0} \frac{dF^*(w+\varepsilon\psi_1, c+\varepsilon\psi_2)}{d\varepsilon} = 0 \ \ \forall \psi_i \quad (i=1,2). \tag{11}$$

From (11), we find, after some manipulations, that

$$\begin{aligned}\delta^{(1)}F^* = \int_{x=0}^{1} [&(k(w_{,xx}-H_0)_{,xx} - q)\psi_1 + (f' - kH_0'(w_{,xx}-H_0)_{,xx} \\ &- k_c c_{,xx} - \mu)\psi_2]dx + k(w_{,xx}-H_0(c))\psi_{1,x}\big|_{x=0}^{1} \\ &+ k(w_{,xx}-H_0(c))_{,x}\psi_1\Big|_{x=0}^{1} + k_c c_{,x}\psi_2\big|_{x=0}^{1}.\end{aligned} \tag{12}$$

where $(\,)'$ indicates derivative of $(\,)$ with respect to c. Since (12) must vanish for any ψ_i, we conclude with the following equilibrium equations:

$$\begin{aligned}&(k(w_{,xx}-H_0))_{,xx} - q = 0 \\ &f' - k_c c_{,xx} - \mu - (kH_0)'(w_{,xx}-H_0) = 0\end{aligned}, \tag{13}$$

subjected to the boundary conditions

$$\begin{aligned}&\text{(a)}\ \ w = 0 && \text{at } x = 0,1 && \text{(zero deflection)} \\ &\text{(b)}\ \ k(w_{,xx}-H_0(c)) = 0 && \text{at } x = 0,1 && \text{(zero bending moment)} \\ &\text{(c)}\ \ c_{,x} = 0 && \text{at } x = 0,1 && \text{(symmetry, zero flux)}\end{aligned} \tag{14}$$

The first equilibrium equation is associated with variation of w, while the second equation with variation of c. Thus, we term these equations *shape equation* and *composition equation*, respectively. Note that the shape equation generalizes the standard bending equation of homogeneous straight beams, and can be rewritten in the form

$$(kw_{,xx})_{,xx} = q + (kH_0)_{,xx}. \tag{15}$$

Thus, $(kH_0)_{,xx}$ can be interpreted as a pseudo load which compensates for the effect of spontaneous curvature. In addition, the first three terms in the composition equation resemble the steady state Cahn Hilliard equation. The fourth term introduces the coupling between shape and composition into the equation.

The shape and composition equations form a set of coupled differential equations. This set is linear with respect to w, yet non-linear in c. Despite the coupling between shape and composition one can rewrite these equations in a form of a nonlinear equation for c only (decoupled from w) along with a coupled equation of c and w. To this end, we integrate the shape equation twice with respect to x:

$$k(w_{,xx}-H_0) = \iint q\,dx + a_1 x + a_0. \tag{16}$$

Above, a_0 and a_1 are integration constants associated with the indefinite integration of q. The values of a_0 and a_1 can be directly calculated from the boundary conditions (14)b:

$$a_0 = -\left(\iint q(x)\right)\Big|_{x=0},\ a_1 = \left(\iint q(x)\right)\Big|_{x=0} - \left(\iint q(x)\right)\Big|_{x=1}. \tag{17}$$

Next, we plug relations (16) and (17) into the composition equation to get

$$\begin{aligned}f' - k_c c_{,xx} - \mu - kH_0'\Bigg(&\iint q(x)dx + \left(\iint q(x)\right)\Big|_{x=0}(x-1) \\ &-\left(\iint q(x)\right)\Big|_{x=1} x\Bigg) = 0,\end{aligned} \tag{18}$$

which is independent of w. For the particular case of a uniform load, $q(x) = q_0$, we write

$$\begin{cases} k(w_{,xx}-H_0) = \frac{1}{2}q_0 x(x-1), \\ f' - k_c c_{,xx} = \frac{1}{2}q_0(kH_0)'x(x-1) + \mu. \end{cases} \tag{19}$$

Therefore, one can calculate equilibrium configurations by solving the second equation, which does not depend on w, for $c(x)$. Then plug the solution for $c(x)$ into the first equation and solve for $w(x)$. The second equation must be solved along with boundary conditions (14)c and the mass constraint (9), while the solution for w must satisfy the boundary conditions (14)a. We emphasize that this "decoupled" procedure is possible only for statically determinate problems, i.e., problems for which the bending moment in the beam can be calculated by means of statics considerations (zero resultant force and moment) only. In particular, it is not possible to obtain a_0 and a_1 directly from the boundary conditions in the case of a statically indeterminate beam.

Recall that the interaction energy, $f(c)$, is a non-linear function of c, which may take a convex (single well) or non-convex (double well) structure depending on temperature. In the Landau formalism $f(c)$ can be approximated by a potential of the form $A_1(T)\cdot(c-c_0)^2 + A_2(T)\cdot(c-c_0)^4$. Plugging this approximation into (18) yields a non-linear ODE (ordinary differential equation) similar to Duffing equation. In particular, if we replace the parameter x with time, equation (18) describes the dynamics of an oscillator subjected to a non-linear potential and a non-harmonic force. Yet, due to this non-harmonic force and boundary conditions (rather than initial conditions in the classical doffing equation) analytical solution (e.g., in terms of elliptic functions) cannot be obtained.

2.3. Stability of equilibrium configuration

The two coupled equations (13) enable us to find equilibrium configurations. Nevertheless, an equilibrium configuration is not necessarily a stable one. We therefore proceed with analyzing the stability of the equilibrium solutions. An equilibrium configuration is said to be stable if the second variation of the energy, calculated at the equilibrium configuration, is positive for any variation in w and c which satisfy the boundary conditions and the mass constraint. In order to formulate stability conditions, two equivalent methods can be applied. (i) In the Lagrange multipliers formalism, stability requires that the second variation of the Lagrange functional, F^*, is positive for any perturbation in w and c *which lie in the space tangent to the constraint* (Zeidler, 1984) and satisfy the boundary conditions. (ii) The complexity associated with the method of Lagrange multipliers can be avoided by introducing variations which satisfy the constraint identically. Below, we adopt the latter method.

In accordance with the second approach above, we introduce the following variations

$$\delta w = \varepsilon\psi_1,\ \ \delta c = \varepsilon\psi_{2,x};\ \ \psi_2(0) = \psi_2(1), \tag{20}$$

for which the mass constraint is satisfied identically:

$$\int_{x=0}^{1}(c+\delta c)\,dx = \int_{x=0}^{1} c\,dx + \int_{x=0}^{1}\psi_{2,x}\,dx = m_I + \psi_2\big|_{x=0}^{x=L} = m_I. \tag{21}$$

Note that the equilibrium equations can also be derived by requiring that the first variation of F vanishes for any variations in w and c of the form (20). This results in a third order differential equation for c, which can be integrated to obtain (19)b. An equilibrium configuration is stable if the second variation of the energy functional, F, is positive for any variations in w and c of the form (20). Therefore, we require that

$$\delta^{(2)}F(w,c) \equiv \lim_{\varepsilon \to 0} \frac{d^2F(w+\varepsilon\psi_1, c+\varepsilon\psi_{2,x})}{d\varepsilon^2} > 0 \ \ \forall \psi_i \neq 0 \quad (i=1,2). \tag{22}$$

Leaving out the details of the calculation we find that

$$\delta^{(2)}F = \sum_{i=1}^{2}\sum_{j=1}^{2}\int_{x=0}^{1} D_{ij}\psi_i\psi_j\,dx. \tag{23}$$

where

$$D_{11}\psi_1\psi_1 = \frac{1}{2}k(\psi_{1,xx})^2. \tag{24}$$

$$D_{12}\psi_1\psi_2 = D_{21}\psi_2\psi_1 = -\frac{1}{2}kH_0'(\psi_{1,xx})^2\psi_{2,x}. \tag{25}$$

$$D_{22}\psi_2\psi_2 = \frac{1}{2}(kH_0''H_0 + f'' + k(H_0')^2 - kH_0''w_{,xx})(\psi_{2,x})^2 + \frac{1}{2}k_c(\psi_{2,xx})^2. \tag{26}$$

Equations (24)–(26) need to be calculated at the specific equilibrium configuration for which stability is examined. Thus, w and c (through $f(c)$ and $H_0(c)$) in the equations above correspond to the solution of the equilibrium equations. The stability condition, (22), along with (24)–(26) provide a powerful tool for numerical analysis of the stability of any equilibrium configuration. Critical configurations are identified by the solution of the eigenvalue problem associated with (23). Further, stability can be examined by studying the eigenvalues of the operator **D.** To this end, we expand ψ_1 and ψ_2 into a series of base functions which satisfy the boundary conditions and condition (20)b, $\psi_2(0) = \psi_2(1)$. Specifically, it is required that

$$\begin{aligned} &\psi_1 = 0 && \text{at } x = 0, 1\\ &\psi_{1,xx} - K_c\psi_{2,x} = 0 && \text{at } x = 0, 1\\ &\psi_{2,xx} = 0 && \text{at } x = 0, 1\\ &\psi_2(0) = \psi_2(1) \end{aligned} \tag{27}$$

where (5) has been used for the second relation. Accordingly, we write

$$\begin{aligned} &\psi_1 = \sum_{n=1}^{\infty} A_n \frac{\phi_n(x)}{\|\phi_n(x)\|}, \quad \psi_2 = B_1 + \sum_{n=3}^{\infty} B_n \frac{\Phi_n(x)}{\|\Phi_n(x)\|}\\ &\phi_1 = x(x-1)(x^2 - x - 1), \quad \phi_2 = x(x-1)(x+2)(3x^2 - 2x - 4)\\ &\phi_n = \Phi_n = (x-1)^3x^n; \quad n \geqslant 3 \end{aligned} \tag{28}$$

An equilibrium solution is stable if the second variation is positive for any A_1, A_2, A_n, B_1, B_n ($n = 3, 4, 5, ..$). After some mathematical manipulations, one can write the second variation in the following form:

$$\delta^{(2)}F = G_{ij}\,v_i\,v_j, \tag{29}$$

where summation convention is used, v_i are the components of the vector of coefficients $v_i = (A_1, A_2, A_3, B_3, A_4, B_4, \ldots)^T$, and **G** is a symmetric matrix. Thus, an equilibrium configuration is stable, if **G** is positive definite. In what follows, all numerical examples involve stable solutions. Further details are provided in Appendix A.

3. Numerical examples

In this Section, we present numerical examples which illustrate the fundamental differences between the mechanical response of beams made of BM compared to "standard" engineering materials. Further, we demonstrate the potential for various engineering applications manifested by these differences. All examples below use the following non-dimensional quantities, in accordance with experimental reports and common experimental set-ups (Baumgart et al., 2005; Boal, 2002; Seifert et al., 1991):

$$k \sim 10^{-19}\ \text{J},\ k_c \sim 10^{-21}\ \text{J},\ K_c = 1\ \mu\text{m}^{-1},\ m_l = 0.5,\ L = 1\ \mu\text{m}, \tag{30}$$

Although in certain systems the dependence of the bending modulus on composition may play an important role (Sorre et al., 2009; Tian et al., 2009), it is usually weaker compared to that of the spontaneous curvature (Seifert, 1997; Sprong et al., 2001). Thus, in the examples below, we neglect the dependence of the bending stiffness with composition and focus our attention to the shape-composition coupling through the spontaneous curvature. In addition, for specificity, we assume a simple model for $f(c)$ which combines aggregation enthalpy and the entropy of mixing:

$$f(c) = k_B\bar{T}\rho_0(c\ln c + (1-c)\ln(1-c)) + \frac{1}{2}B\rho_0 c(1-c), \tag{31}$$

so that it is convex at high temperatures (miscible) but non-convex at low temperatures (immiscible). Above, k_B is Boltzmann constant, and $\bar{T}$ is temperature, and ρ_0 is the density (number of molecules per unit area of the BM). It turns out that the critical temperature, $T_0 = \frac{B}{4k_B}$, is typically close to room-temperature (Veksler and Gov, 2007). Therefore, we rewrite equation (31):

$$f(c) = k_BT_0\rho_0(T(c\ln c + (1-c)\ln(1-c)) + 2c(1-c)), \tag{32}$$

where $T = \bar{T}/T_0$ is a non-dimensional temperature, and

$$T_0 = 297^\circ\ \text{K},\ \ \rho_0 = 10^4\ \mu\text{m}^{-2}. \tag{33}$$

In addition, we consider the following relation for the spontaneous curvature (5):

$$H_0(c) = K_c(c - m_l), \tag{34}$$

which means with no external load ($q_0 = 0$), the beam is straight and has a uniform composition $c(x) = m_l$.

Fig. 3 Illustrates the equilibrium configuration of a beam subjected to a uniform load, $q_0 = 10$ (non-dimensional), directed upward, at a temperature just above T_0. At this temperature the interaction function is $f(c)$ is convex with a single well at $c = 0.5$. Therefore, the composition of the beam tends to be uniform with a value of $c = 0.5$. Nevertheless, the composition is not uniform. This is a direct consequence of the coupling between shape and composition through $H_0(c)$, and exemplifies the fundamental difference between the BM and a standard Cahn–Hilliard system.

Note that even though the variation of composition along the beam is small, it has a significant impact on the beam deflection. Specifically, the 4% dispersion in c leads to a 30% increase in the mid-span deflection compared to the deflection of a standard beam (with constant composition). This implies that BM beams can be "designed" to amplify deflections, which in turn may be exploited for actuation. As temperature is reduced below the critical temperature, the two phases of the BM become less miscible, and tend to form regions with concentrations associated with the two energy wells of $f(c)$, see Fig. 4a. Note the impressive effect that temperature has on the beam deflection (through composition), as illustrated in Fig. 4b. Also, the significant effect of temperature on composition make the BM beam an excellent candidate for non-invasive temperature sensing applications. The two types of domains, each associated with a different energy well of $f(c)$, are separated by continuous "transition" zones - the width of which is controlled by k_c (the gradient term in the energy functional). Fig. 5 illustrates a non-intuitive equilibrium configuration for the same BM at 14 °C below T_0, and a smaller value of k_c, $k_c = 5 \times 10^{-22}$ J. Here, smaller domains form, each with a distinctive composition that is close to a complete separation of the two phases. Consequently, the coupling between shape and composition leads to a non-standard wiggly deflection. Another intriguing behavior of the BM beam is exemplified in Fig. 6 which shows the equilibrium configuration of the same beam from Fig. 5 but with an opposite direction of the external load (same magnitude). Here, contrary to the standard beam, an opposite external

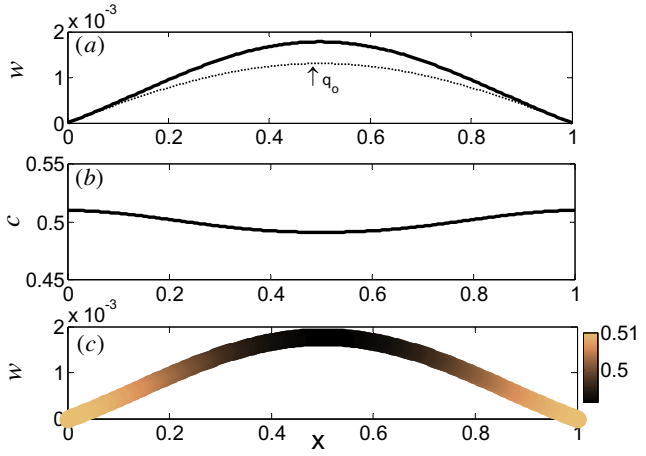

Fig. 3. Equilibrium configuration of a beam subjected to a uniform load, $q_0 = 10$, directed upward, at a temperature slightly above the critical temperature. (a) The deflection of a beam made of BM material (solid line) compared to the deflection expected by a "standard" beam (dashed line). (b) Variation of composition along the beam. (c) Beam configuration – the shape of the curve corresponds to the beam deflection, while the color map illustrates composition.

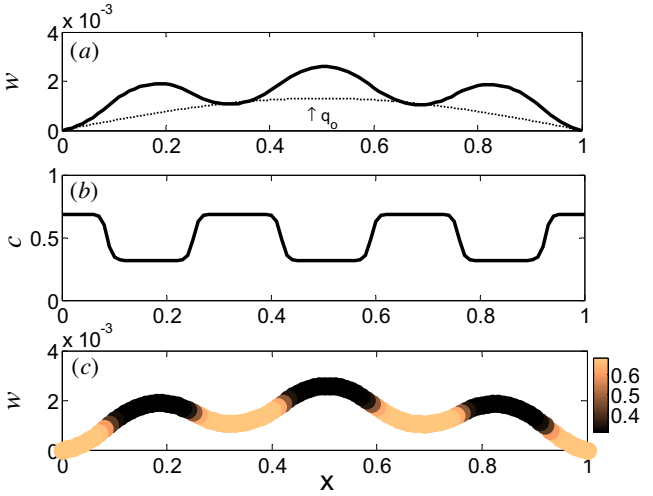

Fig. 5. Equilibrium configuration of a beam subjected to a uniform load, $q_0 = 10$, directed upward, at a temperature of 10 °C, and with $k_c = 5e{-}22$ *J*. (a) The deflection of a beam made of BM material (solid line) compared to the deflection expected by a "standard" beam (dashed line). (b) Variation of composition along the beam. (c) Beam configuration – the shape of the curve corresponds to the beam deflection, while the color map illustrates composition.

load does not invert the beam deflection. Moreover, certain parts of the beam experience deflection that is opposite to the direction of the external load.

The effect of external load is further studied in Fig. 7 which shows the maximum upward deflection as a function of q_0. The kink in the plot corresponds to the load for which the mid-span deflection is equal to the deflection of the incidental regions at the sides (see second inset from the right). Interestingly, it turns out that the level of external load associated with this kink is very

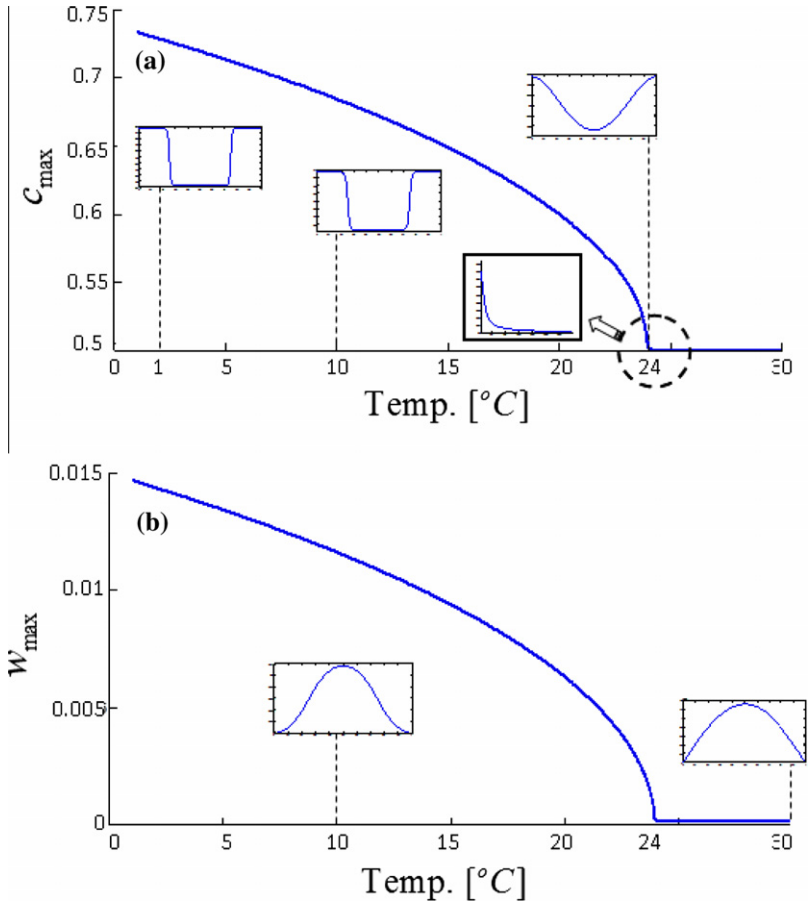

Fig. 4. The effect of temperature on the beam composition and shape. (a) Maximum value of c as function of temperature. Insets show the distribution of c along the beam for 1, 10, 24 °C. (b) Maximum deflection of the beam as a function of temperature. Insets show $w(x)$ for two different 10, 30 °C.

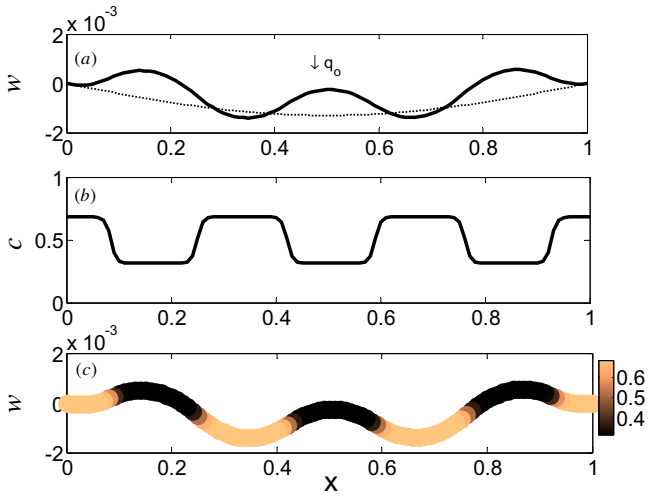

Fig. 6. Equilibrium configuration of a the same beam as in Fig. 5, but the external load is applied downwards. (a) The deflection of a beam made of BM material (solid line) compared to the deflection expected by a "standard" beam (dashed line). (b) Variation of composition along the beam. (c) Beam configuration – the shape of the curve corresponds to the beam deflection, while the color map illustrates composition.

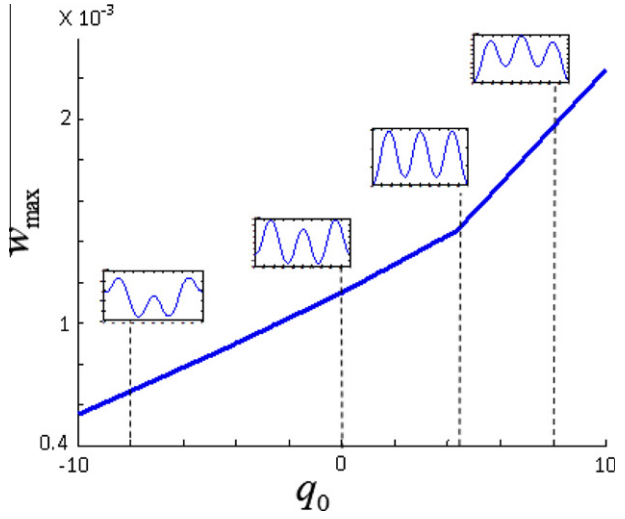

Fig. 7. The effect of the external load on the beam deflection is significantly different from the standard beam. The solids line show the maximal deflection of the beam (upwards) as a function of q_0. Insets show $w(x)$ for four different values of q_0.

sensitive to the value of k_c. Since measuring the value of k_c is a complicated task, Fig. 7 suggests an interesting alternative which enables an indirect measurement of k_c.

4. Summary and conclusions

We have studied a simply supported beam made of a BM-like material comprised from two components. These can represent two different lipid phases (e.g., liquid ordered and liquid disordered phases), two different types of lipid molecules, or mobile membrane proteins embedded in a lipid phase. Equilibrium equations were obtained by calculating the first variation of a generalized Helfrich energy functional subjected to an overall composition constraint. Further, stability of equilibrium configurations was examined by means of the second variation of the energy functional.

We have demonstrated a rich behavior characterized by a variety of non-intuitive equilibrium configurations. Importantly, the coupling between shape and composition make the BM behavior fundamentally different from standard beams and also from standard Cahn–Hilliard systems. The current analysis is limited to small deformations. Extending the current work to account for large deformations is a natural generalization, which will enable us to study the behavior of the structure when subjected to high loads (or osmotic pressure). Obviously, this will result in additional complexity due to geometrical non-linearity.

Our study suggests that BM beams have an interesting potential for sensing and actuation. In particular, local temperature can be measured by means of a simple fluorescence microscopy setup which can be used to measure fluorescence (intensity) of either or both phases. Also, the amplified deflections of the BM can be "designed" for various types of actuation. Such BM applications have inherent advantages which stem from the fact that they are naturally produced by (and exist in) cells. Specifically, the BM is biologically compatible, and attributed to its small size it can provide local sensing and sensitive actuation. Further, current technology enables the design and "production" of artificially made BMs. In addition, the huge variety of different BMs which were optimized by evolution to carry various functions holds a promise for a wide range of possibilities and applications.

Finally, we emphasize that although our study suggests that BMs have the potential to be exploited as smart (biological) materials in engineering applications, such as sensing and actuation, our work is merely theoretical. Whether BMs can practically be used in the way proposed here is an open question. We hope that our results will stimulate such experimental study and motivate further research in this direction.

Acknowledgments

This work was partially supported by the Israel Science Foundation (ISF 1500/10).

Appendix A. The matrix G

After plugging ψ_1 and ψ_2 in the form of (28) into the second variation (23)–(26), we conclude with

$$\delta^{(2)}F = G_{ij}\, v_i\, v_j, \tag{35}$$

where summation convention is used, v_i are the components of the vector of coefficients $v_i = (A_1, A_2, A_3, B_3, A_4, B_4, \ldots)^T$, and $\mathbf{G}$ is a symmetric matrix. The matrix $\mathbf{G}$ takes the following form ($a_i b_j$ does not mean multiplication of a_i with b_j, but is used for association with the corresponding components the vector $\mathbf{v}$):

$$G_{ij} = \begin{pmatrix} a_1a_1 & a_1a_2 & a_1a_3 & a_1b_3 & a_1a_4 & a_1b_4 & \cdots \\ & a_2a_2 & a_2a_3 & a_2b_3 & a_2a_4 & a_2b_4 & \cdots \\ & & a_3a_3 & a_3b_3 & a_3a_4 & a_3b_4 & \cdots \\ & & & b_3b_3 & b_3a_4 & b_3b_4 & \cdots \\ & sym & & & a_4a_4 & a_4b_4 & \cdots \\ & & & & & b_4b_4 & \cdots \\ & & & & & & \cdots \end{pmatrix}, \tag{36}$$

where

$$a_1a_1 = \frac{12}{5}\frac{k}{b^3},\quad a_1a_2 = \frac{1}{2}\frac{204}{5}\frac{k}{b^3},\quad a_2a_2 = \frac{6144}{35}\frac{k}{b^3} \tag{37}$$

and

$$a_1 a_n = \frac{1}{2}\frac{-144k}{(n+4)(n+3)(n+2)(n+1)b^3},$$
$$a_1 b_n = \frac{1}{2}\frac{-72(-3+n)kKc}{(n+5)(n+4)(n+3)(n+2)(n+1)b^2} \tag{38}$$

$$a_2 a_n = \frac{1}{2}\frac{-576(5+4n)k}{(n+5)(n+4)(n+3)(n+2)(n+1)b^3},$$
$$a_2 b_n = \frac{1}{2}\frac{-72(-7n+11n^2-138)kKc}{(n+6)(n+5)(n+4)(n+3)(n+2)(n+1)b^2} \tag{39}$$

$$a_m a_n = \frac{1}{2}\frac{-144(m^2-3mn+1+n^2)nmk}{(m+3+n)(m+2+n)(m+1+n)(m+n)(m-1+n)(m-2+n)(m-3+n)b^3},$$
$$a_m b_n = \frac{1}{2}\frac{36(m-n)(m^2-8mn-3m+2+n^2-3n)kKc}{(m+4+n)(m+3+n)(m+2+n)(m+1+n)(m+n)(m-1+n)(m-2+n)b^2}$$

$$b_m b_n = \frac{1}{2}\left(\begin{array}{l} \frac{-144nmKg(m^2-3mn+1+n^2)}{(m+3+n)(m+2+n)(m+1+n)(m+n)(m-1+n)(m-2+n)(m-3+n)b^3} \\ +\frac{-144kKc^2(m^2+n^2-m-n-3mn)}{b(m+5+n)(m+4+n)(m+3+n)(m+2+n)(m+1+n)(m+n)(m-1+n)} \\ +\int_0^b f''(\frac{x}{b})^m(\frac{x}{b})^n(-x+b)^4(nb-nx-3x)(bm-3x-mx)b^{-6}x^{-2}dx \end{array}\right) \tag{40}$$

For $n, m = 3, 4, 5, \ldots$

References

Altus, E., Givli, S., 2003. Strength reliability of statically indeterminate heterogeneous beams. Int. J. Solids Struct. 40, 2069–2083.

Auth, T., Gompper, G., 2009. Budding and vesiculation induced by conical membrane inclusions. Phys. Rev. E 80.

Baumgart, T., Hess, S.T., Webb, W.W., 2003. Imaging coexisting fluid domains in biomembrane models coupling curvature and line tension. Nature 425, 821–824.

Baumgart, T., Das, S., Webb, W.W., Jenkins, J.T., 2005. Membrane elasticity in giant vesicles with fluid phase coexistence. Biophys. J. 89, 1067–1080.

Bhattacharya, K., James, R.D., 2005. The material is the machine. Science 307, 53–54.

Boal, D.H., 2002. Mechanics of the cell. Cambridge University Press, Cambridge, New York.

Boulbitch, A.A., 1999. Equations of heterophase equilibrium of a biomembrane. Arch. Appl. Mech. 69, 83–93.

Das, S., Tian, A., Baumgart, T., 2008. Mechanical stability of micropipet-aspirated giant vesicles with fluid phase coexistence. J. Phys. Chem. B 112, 11625–11630.

Du, Q., Liu, C., Wang, X.Q., 2004. A phase field approach in the numerical study of the elastic bending energy for vesicle membranes. J. Comput. Phys. 198, 450–468.

Engelman, D.M., 2005. Membranes are more mosaic than fluid. Nature 438, 578–580.

Evans, E.A., Skalak, R., 1980. Mechanics and Thermodynamics of Biomembranes. CRC Press, Boca Raton, Fla.

Feng, F., Klug, W.S., 2006. Finite element modeling of lipid bilayer membranes. J. Comput. Phys. 220, 394–408.

Givli, S., Altus, E., 2003. Effect of strength-modulus correlation on reliability of randomly heterogeneous beams. Int. J. Solids Struct. 40, 6703–6722.

Givli, S., Giang, H., Bhattacharya, K., 2012. Stability of multicomponent biological membranes. SIAM J. Appl. Math. 72, 489–511.

Harden, J.L., MacKintosh, F.C., Olmsted, P.D., 2005. Budding and domain shape transformations in mixed lipid films and bilayer membranes. Phys. Rev. E 72, 011903.

Helfrich, W., 1973. Elastic properties of lipid bilayers – theory and possible experiments. Z. Naturforsch. C 28, 693–703.

Ingber, D.E., 2006. Cellular mechanotransduction: putting all the pieces together again. FASEB J. 20, 811–827.

James, R.D., Hane, K.F., 2000. Martensitic transformations and shape-memory materials. Acta Mater. 48, 197–222.

Julicher, F., Lipowsky, R., 1993. Domain-induced budding of vesicles. Phys. Rev. Lett. 70, 2964–2967.

Kahya, N., Scherfeld, D., Bacia, K., Poolman, B., Schwille, P., 2003. Probing lipid mobility of raft-exhibiting model membranes by fluorescence correlation spectroscopy. J. Biol. Chem. 278, 28109–28115.

Kawakatsu, T., Andelman, D., Kawasaki, K., Taniguchi, T., 1993. Phase-transitions and shapes of 2-component membranes and vesicles. 1. Strong segregation limit. J. Phys. II 3, 971–997.

Kozlov, M.M., Lichtenberg, D., Andelman, D., 1997. Shape of phospholipid/surfactant mixed micelles: Cylinders or disks? Theoretical analysis. J. Phys. Chem. B 101, 6600–6606.

Lowengrub, J.S., Ratz, A., Voigt, A., 2009. Phase-field modeling of the dynamics of multicomponent vesicles: Spinodal decomposition, coarsening, budding, and fission. Phys. Rev. E 79, 13.

Ma, L., Klug, W.S., 2008. Viscous regularization and r-adaptive remeshing for finite element analysis of lipid membrane mechanics. J. Comput. Phys. 227, 5816–5835.

Parthasarathy, R., Yu, C.H., Groves, J.T., 2006. Curvature-modulated phase separation in lipid bilayer membranes. Langmuir 22, 5095–5099.

Perozo, E., Rees, D.C., 2003. Structure and mechanism in prokaryotic mechanosensitive channels. Curr. Opin. Struct. Biol. 13, 432–442.

Safran, S.A., Pincus, P.A., Andelman, D., Mackintosh, F.C., 1991. Stability and phase-behavior of mixed surfactant vesicles. Phys. Rev. A 43, 1071–1078.

Samsonov, A.V., Mihalyov, I., Cohen, F.S., 2001. Characterization of cholesterol-Sphingomyelin domains and their dynamics in bilayer membranes. Biophys. J. 81, 1486–1500.

Seifert, U., 1993. Curvature-induced lateral phase segregation in 2-component vesicles. Phys. Rev. Lett. 70, 1335–1338.

Seifert, U., 1997. Configurations of fluid membranes and vesicles. Adv. Phys. 46, 13–137.

Seifert, U., Berndl, K., Lipowsky, R., 1991. Shape transformations of vesicles – phase-diagram for spontaneous-curvature and bilayer-coupling models. Phys. Rev. A 44, 1182–1202.

Singer, S.J., Nicolson, G.L., 1972. The fluid mosaic model of the structure of cell membranes. Science 175, 720–731.

Sorre, B., Callan-Jones, A., Manneville, J.B., Nassoy, P., Joanny, J.F., Prost, J., Goud, B., Bassereau, P., 2009. Curvature-driven lipid sorting needs proximity to a demixing point and is aided by proteins. PNAS 106, 5622–5626.

Sprong, H., van der Sluijs, P., van Meer, G., 2001. How proteins move lipids and lipids move proteins. Nat. Rev. Mol. Cell Biol. 2, 504–513.

Stamenovic, D., Wang, N., 2000. Cellular Responses to Mechanical Stress: Invited Review: Engineering approaches to cytoskeletal mechanics. J. Appl. Physiol. 89, 2085–2090.

Swanson, C.P., Webster, P.L., 1977. The cell, fourth ed. Prentice-Hall, Englewood Cliffs, NJ.

Tian, A.W., Capraro, B.R., Esposito, C., Baumgart, T., 2009. Bending stiffness depends on curvature of ternary lipid mixture tubular membranes. Biophys. J. 97, 1636–1646.

Veatch, S.L., Keller, S.L., 2003. Separation of liquid phases in giant vesicles of ternary mixtures of phospholipids and cholesterol. Biophys. J. 85, 3074–3083.

Veksler, A., Gov, N.S., 2007. Phase transitions of the coupled membrane-cytoskeleton modify cellular shape. Biophys. J. 93, 3798–3810.

Vogel, V., Sheetz, M., 2006. Local force and geometry sensing regulate cell functions. Nat. Rev. Mol. Cell Biol. 7, 265–275.

Yanagisawa, M., Imai, M., Taniguchi, T., 2010. Periodic modulation of tubular vesicles induced by phase separation. Phys. Rev. E 82, 051928.

Zeidler, E., 1984. Non-Linear Functional Analysis and its Applications. Springer-Verlag, New-York.

Zhong-can, O.-Y., Helfrich, W., 1989. Bending energy of vesicle membranes: General expressions for the first, second, and third variation of the shape energy and applications to spheres and cylinders. Phys. Rev. A 39, 5280.

Zhu, C., Bao, G., Wang, N., 2000. Cell mechanics: mechanical response, cell adhesion, and molecular deformation. Annu. Rev. Biomed. Eng. 2, 189–226.